Testing linear models on spectral daylight measurements

Javier Hernández-Andrés, Javier Romero, Antonio García-Beltrán, and Juan L. Nieves

We have analyzed the results of the reconstruction quality of 252 daylight spectral curves measured at Granada, Spain, using four bases obtained from measurements in different areas of the world. For these reconstructions we used two different methods (orthogonality of characteristic vectors and chromaticity coordinates) to study the influence of the wavelength range and spectral resolution. The reconstruction method from chromaticity coordinates presents difficulties for the spectral recovery of daylight spectral power distributions regardless of the basis used. The orthogonality method makes clear that the best bases were those proposed by the CIE, but more than two characteristic CIE vectors were needed for good reconstruction. © 1998 Optical Society of America

OCIS codes: 330.6180, 010.0010.

1. Introduction

Detailed knowledge of the spectral power distributions (SPD's) of daylight in the visible and ultraviolet regions of the spectrum has many applications in science (atmospheric optics, meteorology, medicine, biology, etc.), technical areas (photovoltaic applications, biomass production, color rendering and metamerism, agriculture, architecture, etc.), and industry (photography, dyes, paintings, textile, etc.). In addition, algorithms that enable the color identification and recognition in Artificial Vision[1–3] have been developed by use of mathematical properties found for daylight SPD's.

In the 1960's and 1970's, thanks to complex instruments capable of measuring spectral distributions of daylight, measurement campaigns were conducted in different countries (U.S.A., England, Japan, India, South Africa, Australia).[4–10] Some of this research achieved great precision and elaboration. The main objective was to standardize, for practical purposes, the representative spectral distributions of daylight. The principal conclusion drawn from all these campaigns was that, despite the large number of factors that influence the daylight SPD's (solar elevation, altitude, atmospheric conditions, receptor position, etc.), SPD variability is low, so the daylight spectral distributions present strong correlation.

Taking advantage of this strong correlation, we can use a linear basis expansion of the SPD's to represent the daylight by a linear model with fixed, known basis lights. With regard to the accuracy with which a linear model captures the range of spectral variation of daylight, various authors[4–9] have determined that, for practical purposes, three to four basis lights provide essentially acceptable matches to the spectral distributions measured when bases are tested on the author's own measurements.

Here we outline the possibilities of the various bases (one a CIE basis[4] recommended by the scientific community[11]) to represent daylight SPD's measured in a different place. We also obtained a basis from our own measurements to evaluate the goodness of the different bases tested, as it might be thought that a Granada basis would provide a better reconstruction of them than would another basis deduced from other measurements. Our basis was obtained by a principal components analysis.

In an early paper, Nayatani *et al.*,[10] after measuring 112 SPD's of daylight in Amagasaki, Japan, compared their curves with those reconstructed by the method recommended by the CIE-1.3.1. Committee. These authors found fairly good agreement in the visible region but larger discrepancies in the ultraviolet region. To evaluate the goodness of their reconstructions, Nayatani *et al.*[10] used the coefficient ${}_BM_t$ of the degree of metamerism proposed by Nimeroff and Yurow,[12] as they were more interested in colorimetric aspects than in spectral reconstruction.

The authors are with the Departamento de Optica, Facultad de Ciencias, Universidad de Granada, Granada 18071, Spain.

Received 4 March 1997; revised manuscript received 11 July 1997.

0003-6935/98/060971-07$10.00/0

We analyzed two different methods for the recovery of the SPD's: in one the curves were reconstructed knowing the chromaticity coordinates of the daylight SPD, and in the other they were reconstructed using the orthogonality properties of the characteristic vectors deduced from a set of daylight measurements. With the second method, since we wondered whether the bases deduced far from Granada would serve to reconstruct Granada daylight SPD's, we studied which method provides the best results and what is the appropriate dimension of this basis and its possibilities for representing daylight SPD's. We also studied the influence on the spectral quality of different reconstruction parameters, such as wavelength range and spectral resolution, vectors used and their orthogonality, and interpolations and their truncation.

Four different bases were tested. The first basis used was formed by the characteristic vectors calculated by Judd *et al.*[4] from a set of 622 samples of natural daylight composed of three subsets measured in different widely scattered places: 249 spectral distributions from Rochester, New York, supplied by Condit and Grum[7]; 274 from Enfield, England, supplied by Henderson and Hodgkiss[8]; and 99 from Ottawa, Canada, supplied by Budde. The authors published the mean and the first four characteristic vectors, using the method described by Simonds,[13] for the 330–700-nm range every 10 nm. In that same paper these authors extended their vectors to cover the wavelength ranges of 300–330 and 700–830 nm, using Moon's compilation data[14] on the spectral transmission of the Earth's atmosphere that is due to ozone and water vapor. The CIE recommended a procedure,[11] based on this work, to specify relative spectral radiant power distributions of typical phases of daylight at the Earth's surface for correlated color temperatures (CCT's) ranging from 4000 to 25,000 K. We have designated the characteristic vectors of Judd *et al.*[4] as the CIE characteristic vectors, since their research was the basis of the actual CIE Standard Daylight Illuminants. It should be mentioned that a redefinition of the CIE Standard Daylight Illuminant spectral power distribution is currently under consideration. The CIE TC 2-33, "Re-formulation of CIE Standard Illuminants A and D65," is preparing a new edition of CIE Standard S001-1986 (now ISO/CIE 10526).[15]

The second basis was taken from Sastri and Das,[5] who presented 187 spectral distributions of daylight at Delhi, India, recorded for approximately a year. They gave the mean and the first four characteristic vectors for the 300–700-nm range every 10 nm. Their reconstructions of typical distributions for five CCT's using the mean and the first two characteristic vectors show satisfactory agreement except in the 300–330-nm range. From their results these authors concluded that their values for this range did not lead to a representative mean or characteristic vectors, affirming that "the sensitivity of our measuring system was rather poor for this range."[5]

The third and fourth bases were published by Dixon.[6] He took measurements of the spectral distributions of Australian daylight falling on a horizontal plane over the 280–2800-nm wavelength range at two locations in southeastern Australia, one in an urban environment, Coburg, and the other in the country, Bendigo. Each set (123 curves for Bendigo and 113 for Coburg) was subjected to characteristic vector analysis. All the tabulations of spectral data in Dixon's work were at "rather odd wavelengths."[6] The recorded wavelengths of the visible monochromator were different for Bendigo and Coburg. The range of the vectors for the Bendigo data was 264.4–782.7 nm and for Coburg it was 264.4–780.6 nm.

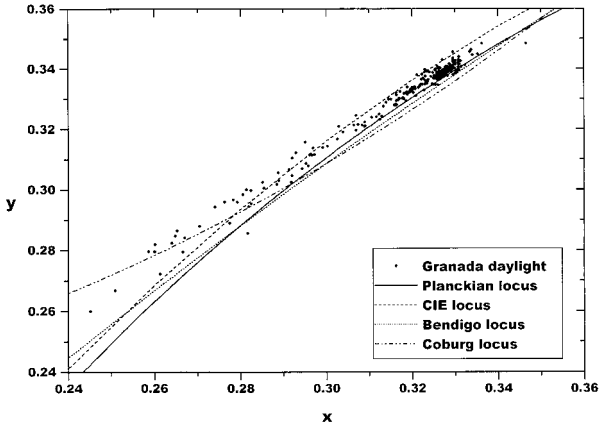

Fig. 1. Chromaticity of Granada daylight on the 1931 CIE chromaticity diagram.

2. Experimental Measurements

We measured 252 spectral distributions of daylight (sunlight plus skylight) at Granada, Spain. This set of measurements was made from a flat roof of the Science Faculty of the University of Granada (latitude 37°11′N, longitude 3°35′W, altitude 680 m), situated within a nonindustrial area of the city of Granada in southern Spain. The data set was compiled for 30 days, from 9 February to 3 May 1996, and it covered a full range of atmospheric conditions: clear sky, scattered clouds, cloudy, hazy, overcast,

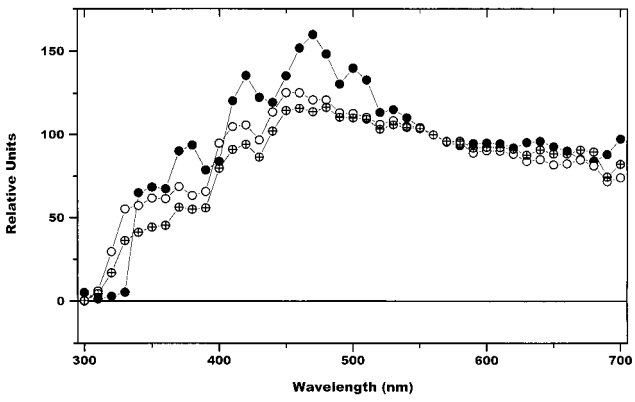

Fig. 2. Spectral profiles of the CIE (open circles), Sastri and Das (solid circles) mean vectors, and the Granada (crossed circles) first eigenvector in the 300–700-nm spectral range with a spectral resolution of 10 nm.

Table 1. Coefficient Values for Eqs. (2) and (3)

	Basis			
Coefficients	CIE	Sastri and Das	Bendigo	Coburg
a_1	−1.3515	−1.3917	14.5420	−167.6472
a_2	−1.7703	0.4941	154.0998	−3.1582
a_3	5.9114	4.0524	−193.0454	504.0529
c_1	0.0241	1.0000	−1.0000	−1.0000
c_2	0.2562	−14.3022	21.4735	−120.7553
c_3	−0.7341	2.9761	7.1238	54.4907
b_1	0.0300	−1.0915	4.1075	−55.3406
b_2	−31.4424	−22.2796	−1112.9636	−8118.4574
b_3	30.0717	25.1195	1061.0842	8066.8239

misty, etc. The measurements were taken from sunrise to sunset at intervals of 1 h, with a Licor LI-1800 scanning spectroradiometer[16] that was used to scan the 300–1100-nm wavelength range (sampling every 1 nm) at 40 s/scan.

Figure 1 presents the chromaticity coordinates of our 252 curves: the CIE daylight locus, the Bendigo locus and Coburg locus, as well as the Planckian locus. Most of the Granada data with small CCT are located above the Planckian locus (toward the green region) and below the CIE locus. However, for larger CCT's our chromaticity coordinates are located above the CIE locus.

The analytic method used to obtain the eigenvectors from the 252 curves of Granada data are described in Parkkinen *et al.*[17] and Romero *et al.*[18] The data were analyzed by using the Karhunen–Loève transformation, which is closely related to the principal component analysis. These eigenvectors are mutually orthogonal and may have negative values, but they do not have equal importance in spectral representation. The first eigenvector corresponds to the mean of the measured vector.

Figure 2 shows the spectral profiles of the CIE, the Sastri and Das mean vectors, and the Granada first eigenvector in the 300–700-nm spectral range. The CIE mean vector and that of Granada share similar spectral profiles, particularly for wavelengths above 500 nm. These vectors differ markedly from those of Sastri and Das for wavelengths below 500 nm. The UV content in the CIE mean vector and in the Sastri and Das mean vector (over 330 nm) exceeds that at Granada.

3. Reconstruction Methods

As mentioned above, we analyzed the way in which the reconstruction method could influence the quality of spectral reconstruction. We chose two different methods. In the first, we must know the chromaticity coordinates of the original curve; with this knowledge, together with the mean vector and the first two characteristic vectors, we can reconstruct the desired curve. In the other method we used the orthogonality properties that the characteristic vectors must fulfill, and we had no limit on the number of vectors used.

A. Reconstruction from Chromaticity Coordinates

With this method the reconstructed SPD $[E_R(\lambda)]$ is obtained by the expression

$$E_R(\lambda) = E_1(\lambda) + M_1 V_1(\lambda) + M_2 V_2(\lambda), \tag{1}$$

where $E_1(\lambda)$ is the mean vector, and $V_1(\lambda)$ and $V_2(\lambda)$ are the first two characteristic vectors.

Judd *et al.*[4] developed the following expression relating the scalar multiples M_1 and M_2 to the chromaticity coordinates x and y of the curve they wished to reconstruct:

$$M_1 = \frac{a_1 + a_2 x + a_3 y}{c_1 + c_2 x + c_3 y}, \tag{2}$$

$$M_2 = \frac{b_1 + b_2 x + b_3 y}{c_1 + c_2 x + c_3 y}. \tag{3}$$

We obtained similar expressions for the three remaining bases and the results are shown in Table 1. The major limitation of this method is that, if we wish the reconstructed curve to be unique, i.e., a univocal relationship between chromaticities and scalar multiples, we can use only two characteristic vectors, but these two vectors may not cover all the variability in the daylight spectrum.

B. Reconstruction Using the Orthogonality Property

This procedure is based on the orthogonality of the characteristic vectors V_j, which represent statistically independent types of response variability. Mathematically stated,

$$\langle V_a | V_b \rangle = 0 = \sum_i V_a(\lambda_i) V_b(\lambda_i) \qquad a \neq b. \tag{4}$$

Table 2. Average GFC for the 252 Curves from *x*, *y* Data with Different Bases, Spectral Ranges, and Spectral Resolutions[a]

	Spectral Range and Spectral Resolution							
Studies	300–700 nm		300–780 nm		330–700 nm		300–830 nm	
Basis	10 nm	5 nm	10 nm	5 nm	10 nm	5 nm	10 nm	5 nm
CIE	0.99615	0.99615	0.99538	0.99505	0.99632	0.99638	0.99500	0.99476
Sastri and Das	0.98701	0.98851	n.a.	n.a.	0.98755	0.98984	n.a.	n.a.
Bendigo	0.99561	0.99586	0.99434	0.99462	0.99658	0.99696	n.a.	n.a.
Coburg	0.99294	0.99338	0.95342	0.95891	0.99354	0.99416	n.a.	n.a.

[a]n.a., not available.

Table 3. Percentage of Reconstructions (from *x*, *y* Data) that Surpass a Given GFC Value[a]

Studies	Spectral Range							
	300–700 nm		300–780 nm		330–700 nm		300–830 nm	
Basis	≥0.99	≥0.999	≥0.99	≥0.999	≥0.99	≥0.999	≥0.99	≥0.999
CIE	96.4	0	95.2	0	96.8	0	94.4	0
Sastri and Das	45.6	0	n.a.	n.a.	66.7	0	n.a.	n.a.
Bendigo	91.7	34.5	88.5	28.6	94.8	42.5	n.a.	n.a.
Coburg	82.9	37.7	23.0	1.6	83.7	40.5	n.a.	n.a.

[a]Spectral resolution: 5 nm; n.a., not available.

For the mathematical reconstruction of a spectral power distribution $E_E(\lambda)$ from the mean vector and p characteristic vectors, we used the formula

$$E_R(\lambda) = E_1(\lambda) + \sum_{j=1}^{p} \langle E_E(\lambda)|V_j(\lambda)\rangle V_j(\lambda), \qquad (5)$$

where $\langle E_E(\lambda)|V_j(\lambda)\rangle$ is the usual inner product (scalar product) between the spectral power distribution and the j-basis characteristic vector, $E_1(\lambda)$ is the mean vector, $E_R(\lambda)$ is the reconstructed curve, and p is the number of characteristic vectors with which we wish to recover the spectral distribution.

When we use the eigenvectors calculated from the Karhunen–Loève transformation (only for the Granada data), the formula is slightly different since the mean vector is not used:

$$E_R(\lambda) = \sum_{i=1}^{p} \langle E_E(\lambda)|W_i(\lambda)\rangle W_i(\lambda), \qquad (6)$$

where $W_i(\lambda)$ indicates the ith eigenvector.

4. Goodness Evaluation

To evaluate the goodness of the mathematical reconstruction, we used a goodness-fitting coefficient (GFC) based on the inequality of Schwartz:

$$\mathrm{GFC} = \frac{\left|\sum_j E_E(\lambda_j) E_R(\lambda_j)\right|}{\left|\sum_j [E_E(\lambda_j)]^2\right|^{1/2} \left|\sum_j [E_R(\lambda_j)]^2\right|^{1/2}}. \qquad (7)$$

This GFC is the multiple correlation coefficient R, and the square root of the variance accounted for. The GFC ranges from 0 to 1, where 1 indicates a perfect reconstruction. When the reconstruction presented a GFC ≥ 0.99, we judged the quality to be acceptable, especially from the standpoint of colorimetry as done by Romero *et al.*[18] When the GFC obtained was ≥0.999 the reconstruction was considered very good, and ≥0.9999 was almost exact.

5. Spectral Range and Spectral Resolution

Because a different spectral range and spectral resolution is given by the authors[4–6] for each basis, we selected four different spectral ranges (300–700, 300–780, 330–700, and 300–830 nm) with two spectral resolutions (10 and 5 nm) in order to compare the results and to determine the influence of these two parameters on the quality of the reconstructed curves.

A SPD with N samples can be considered as a vector with dimension N. For example, a daylight curve in the 400–700-nm wavelength range with a spectral resolution of 10 nm is a vector with a dimension of 31. Therefore, widening the spectral range or reducing the sampling gap increases the dimensionality of the vectors used, thereby multiplying the possibilities of variability in the spectral profiles of the curves. After we used vectors defined every 10 nm, we made a linear interpolation to determine the values every 5 nm. This same interpolation was made for the Bendigo and Coburg vectors (Dixon[6]) because their spectral data were at unconventional wavelengths. In the same way, when the spectral range studied was less than the original spectral range of the vectors, we limited the calculation of the GFC to the smaller spectral range, calculating the inner product in the original spectral range. In the tables these results appear in italics. The Granada vectors were calculated at four wavelength ranges (300–700, 300–780, 330–700, and 300–830 nm) with two spectral resolutions (5 and 10 nm), performing eight eigen analyses over eight different matrices.

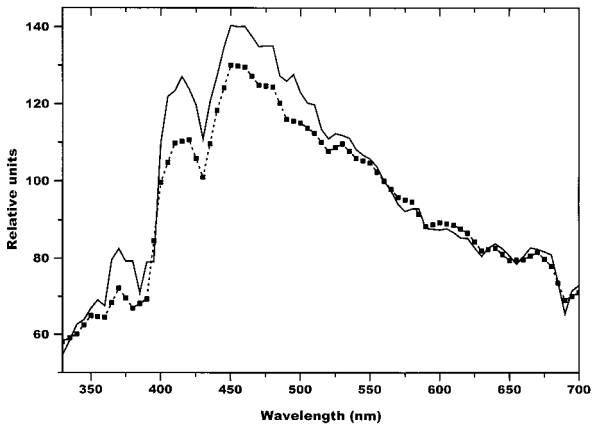

Fig. 3. Example of reconstruction from the chromaticity coordinates by use of the CIE basis with a GFC of 0.9987 in the 330–700-nm spectral range with a spectral resolution of 5 nm. Solid curve, original curves; squares connected by dotted curve, reconstruction.

Table 4. Average GFC for the 252 Curves by use of Orthogonality[a]

Studies	Spectral Range and Spectral Resolution							
	300–700 nm		300–780 nm		330–700 nm		300–830 nm	
Basis	10 nm	5 nm	10 nm	5 nm	10 nm	5 nm	10 nm	5 nm
CIE [2]	*0.99744*	*0.99795*	*0.99729*	*0.99734*	0.99855	0.99848	0.99751	0.99715
CIE [3]					0.99963	0.99951		
CIE [4]					0.99977	0.99964		
Sastri and Das [2]	0.99088	0.99407	n.a.	n.a.	*0.99115*	*0.99441*	n.a.	n.a.
Sastri and Das [3]	0.99124	0.99435			*0.99150*	*0.99467*		
Sastri and Das [4]	0.99129	0.99440			*0.99155*	*0.99469*		
Bendigo [2]	0.73422	0.72321	0.76604	0.75941	*0.74275*	*0.73626*	n.a.	n.a.
Bendigo [3]	0.62875	0.60401	0.75072	0.74807	*0.64284*	*0.62713*		
Coburg [2]	0.90833	0.91006	0.93758	0.94555	*0.90928*	*0.91106*	n.a.	n.a.
Coburg [3]	0.49860	0.49729	0.67643	0.69886	*0.51619*	*0.52204*		
Coburg [4]	0.48197	0.48069	0.65940	0.67416	*0.50235*	*0.50993*		
Granada [2]	0.99932	0.99933	0.99910	0.99910	0.99939	0.99942	0.99904	0.99904
Granada [3]	0.99978	0.99979	0.99959	0.99960	0.99980	0.99981	0.99954	0.99954
Granada [4]	0.99994	0.99994	0.99984	0.99984	0.99995	0.99995	0.99982	0.99982
Granada [5]	0.99996	0.99996	0.99991	0.99991	0.99998	0.99998	0.99990	0.99990
Granada [6]	0.99998	0.99998	0.99996	0.99996	0.99998	0.99999	0.99996	0.99996

[a]For bases formed by characteristic vectors, the number of characteristic vectors used is indicated in brackets (without including the mean vector); in the Granada basis, the number in brackets indicates the number of eigenvectors. When we calculated the GFC in a spectral range smaller than that used for the inner product, the results are in italic; n.a., not available.

6. Results

A. Reconstruction from Chromaticity Coordinates

From the chromaticity coordinates of our measurements, we reconstructed 252 spectral curves using the four bases described in Section 1 as well as expressions (1)–(3). We calculated the average GFC (Table 2) at four spectral ranges with two spectral resolutions. Table 3 lists the percentage of reconstructions that surpassed a given GCF value for those four spectral ranges with a spectral resolution of 5 nm and we found similar results for a spectral resolution of 10 nm.

The CIE basis, as well as Bendigo and Coburg bases, provides the best average GFC results (except for the Coburg basis between 300 and 780 nm for which the results are discouraging). The differences between these three bases and that of Sastri and Das are significant, with the latter rendering the worst results. Although the CIE basis provides the best GFC averages, we found that no reconstruction (of the 252 analyzed) had a GFC greater than 0.999. However, with the Bendigo and Coburg bases roughly 30% of the reconstructions had a GFC of greater than 0.999 (except between 300 and 780 nm for the Coburg basis). Again, the Sastri and Das basis gave the worst results.

We found that reducing the size of the spectral range increased the average GFC. This trend was true for all the bases, and particularly so for the

Table 5. Percentage of Reconstructions from Orthogonality Properties that Surpass a Given GFC Value[a]

Studies	Spectral Range											
	300–700 nm			300–780 nm			330–700 nm			300–830 nm		
Basis	≥0.99	≥0.999	≥0.9999	≥0.99	≥0.999	≥0.9999	≥0.99	≥0.999	≥0.9999	≥0.99	≥0.999	≥0.9999
CIE [2]	*95.2*	*71.0*	*0*	*95.2*	*33.3*	*0*	96.8	81.0	0	95.2	11.1	0
CIE [3]	n.a.	n.a.	n.a.	n.a.	n.a.	n.a.	100	92.9	0	n.a.	n.a.	n.a.
CIE [4]	n.a.	n.a.	n.a.	n.a.	n.a.	n.a.	100	99.2	0	n.a.	n.a.	n.a.
Sastri and Das [2]	97.6	0	0	n.a.	n.a.	n.a.	*98.8*	*0*	*0*	n.a.	n.a.	n.a.
Sastri and Das [3]	99.6	0	0	n.a.	n.a.	n.a.	*99.6*	*0*	*0*	n.a.	n.a.	n.a.
Sastri and Das [4]	99.6	0	0	n.a.	n.a.	n.a.	*99.6*	*0*	*0*	n.a.	n.a.	n.a.
Granada [2]	98.8	83.7	27.0	98.8	79.0	7.1	99.2	87.7	35.3	99.2	78.2	5.2
Granada [3]	99.6	97.6	61.5	99.2	93.7	23.4	100	97.6	65.1	99.6	90.5	19.4
Granada [4]	100	99.2	90.1	99.6	99.2	64.3	100	99.6	94.8	99.6	98.8	59.1
Granada [5]	100	99.2	95.6	100	99.6	84.1	100	100	98.0	100	99.6	80.2
Granada [6]	100	100	98.8	100	100	94.8	100	100	98.8	100	100	94.0

[a]Spectral resolution: 5 nm; n.a., not available. For bases formed by characteristic vectors, the number of characteristic vectors used is indicated in brackets (without including the mean vector); in the Granada basis, the number in brackets indicates the number of eigenvectors. When we calculated the GFC in a spectral range smaller than that used for the inner product, the results are in italic.

Coburg basis when analyzed between 300 and 780 nm, where the deterioration was clear. This trend also becomes evident in each basis for which a change in the spectral resolution from 10 to 5 nm (in curves and vectors) slightly increased the average GFC.

With this method, which allows the recovery of daylight SPD using three vectors (mean vector and two characteristic vectors) and knowing its chromaticity coordinates, we obtain poor spectral quality regardless of the basis used. Although this method by use of the CIE basis is widely employed for standard daylight, it has been shown that it is not advisable if we are concerned about spectral similarities. Figure 3 shows an example of reconstruction that was obtained with this method with the CIE basis, resulting in a GFC of 0.9987.

B. Reconstruction Using the Orthogonality Property

We calculated the average GFC (Table 4) and the percentage of reconstructions that surpassed a given GCF value (Table 5). These results show that an increase in the number of vectors in the Sastri and Das basis did not increase the GFC as appreciably as when the CIE basis was used, perhaps because the Sastri and Das vectors do not cover the variability found in the spectral curves of Granada daylight. For the CIE vectors, despite increasing the number of characteristic vectors to four, in the 330–700-nm spectral range no curve exceeded a GFC of 0.9999. However, with only two characteristic vectors a large majority (81%) reached the quality of very good (GFC $\geq$ 0.999).

Table 5 also reveals that no reconstruction with the Sastri and Das basis surpassed the quality of very good, despite the increase of the number of vectors to four. Nevertheless, approximately 98% of the reconstructions qualified as acceptable, even with two characteristic vectors. This percentage was lower (95%) for the CIE vectors.

Using two Granada eigenvectors, most of the reconstructions (roughly 80%) surpass the quality of very good in the four spectral ranges (Table 5). Three eigenvectors are needed for more than half of the reconstructions to surpass the quality of excellent for the ranges (300–700 and 330–700 nm), and four are needed for the widest ranges (300–780 and 300–830 nm). With six eigenvectors, almost the entire set of reconstructions (~98%) surpassed the quality of excellent. Figures 4(a) and 4(b) show two reconstructions using the CIE basis and Granada basis, resulting in GFC's of 0.99925 and 0.99996, respectively.

The broader the spectral range, the lower the quality of the reconstructions (similar results were found when the reconstructions were made from the chromaticity coordinates). When we included the 300–330-nm spectral range (UV A and part of UV B), far smaller than 700–780 or 700–830 nm, more quality was lost than when we included these ranges. We can increase the GFC of reconstructions eliminating this spectral range (300–330 nm) where the ozone concentrations varied seasonally and locally from one region to another, when the measuring instruments had low sensitivity, and where there is little correlation.

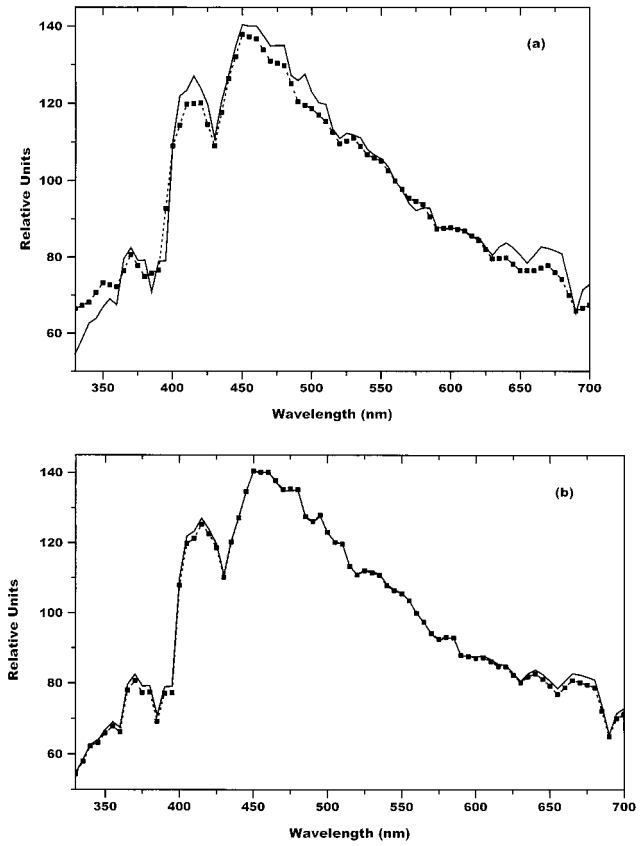

Fig. 4. (a) Example of reconstruction from the orthogonality properties by use of the CIE mean and first two characteristic vectors with a GFC of 0.99925 in the 330–700-nm spectral range with a spectral resolution of 5 nm. Solid curve, original curves; squares connected by dotted curve, reconstruction. (b) Example of reconstruction from the orthogonality properties by use of the Granada first three eigenvectors with a GFC of 0.99996 in the 330–700-nm spectral range with a spectral resolution of 5 nm. Solid curve, original curves; squares connected by dotted curve, reconstruction.

As explained above, the reconstructions were made using the orthogonality of the characteristic vectors expressed in Eq. (4). If this property is lost, that is, if the scalar product between characteristic vectors is not near 0, then the reconstructed curves do not resemble the originals. Several factors could contribute to orthogonality loss; for example, vector values with fewer than four figures supplied by other authors,[4–6] and this precision has a negative influence on the orthogonality property that vectors must fulfill, reducing the GFC's obtained when one uses this method. Surprisingly the linear interpolations made to change the spectral resolution from 10 to 5 nm improved the quality of the reconstructions even though the orthogonality worsened.

Judd *et al.*,[4] using Moon's compilation,[14] extrapolated the mean vector and the first two characteristic vectors to the ranges of 300–330 and 700–830 nm. The orthogonality between these characteristic vec-

tors was considerably smaller than for the original 330–700-nm range (e.g., the dot product between V_1 and V_2 changes from 0.00069 in the original range to 0.12784 in the extrapolated 300–830-nm range). This result is faintly reflected by the average GFC obtained for this range (300–830 nm) compared with that obtained for 330–700 nm (Table 4).

The orthogonality was reduced sharply when the original vectors (Bendigo as well as Coburg) were truncated in the intervals studied (the original range of which had wavelengths of less than 300 nm). This loss of orthogonality is reflected in the results of the average GFC: the GFC decreases despite our increase of the number of characteristic vectors used in the reconstructions (Table 4). Therefore, with the orthogonality method it is not advisable to truncate the spectral ranges of vectors when we use vectors defined for spectra wider than those for which we wish to make the reconstructions.

This method of reconstruction of daylight SPD supplies better results in the spectral quality of reconstructions than the one that makes use of the chromaticity coordinates. However, if we want high spectral quality we must use a number of vectors greater than four.

7. Conclusions

It is a fact that the algorithms that enable the color identification and recognition in Artificial Vision use reconstructions of daylight SPD's with linear models. Therefore, it is essential to study from a spectral standpoint the quality of reconstructions, testing to which degree different bases can be used to reconstruct daylight spectral curves that have been measured at sites that were different from the original ones. We have shown that the reconstruction method from chromaticity coordinates presents difficulties for the spectral representation of daylight SPD's, regardless of the basis used. The orthogonality method points out that the best basis and the one that most effectively reconstructed the spectral curves of Granada daylight was that proposed by the CIE. The differences with respect to other bases were quite noticeable. We should emphasize that more than two characteristic CIE vectors were needed for good reconstruction, since two (and the mean vector) gave acceptable results only from a colorimetric standpoint.

We also determined that use of a spectral resolution of 5 nm (as opposed to 10 nm) improves the quality of the reconstructions for the two methods described above. This result, perhaps at first unexpected, is notable because to increase the spectral resolution one must multiply the dimension of the vectors by two, and since this implies a loss in the orthogonality property we might thus expect a worsening of the GFC because it would cover greater variability in the SPD's. This result can be explained by the fact that an increase in the spectral resolution implies great specification in the spectral location of the absorption bands (water vapor, oxygen, ozone, aerosols, etc.).

References and Notes

1. B. A. Wandell, "The synthesis and analysis of color images," IEEE Trans. Pattern Anal. Mach. Intell. **PAMI-9,** 2–13 (1987).
2. L. T. Maloney and B. A. Wandell, "Color constancy: a method for recovering surface spectral reflectance," J. Opt. Soc. Am. A **3,** 29–33 (1986).
3. D. H. Marimont and B. A. Wandell, "Linear models of surface and illuminant spectra," J. Opt. Soc. Am. A **9,** 1905–1913 (1992).
4. D. B. Judd, D. L. MacAdam, and G. Wyszecki, "Spectral distribution of typical daylight as a function of correlated color temperature," J. Opt. Soc. Am. **54,** 1031–1040 (1964).
5. V. D. P. Sastri and S. R. Das, "Typical spectral distributions and color for tropical daylight," J. Opt. Soc. Am. **58,** 391–398 (1968).
6. E. R. Dixon, "Spectral distribution of Australian daylight," J. Opt. Soc. Am. **68,** 437–450 (1978).
7. H. R. Condit and F. Grum, "Spectral energy distribution of daylight," J. Opt. Soc. Am. **54,** 937–944 (1964).
8. S. T. Henderson and D. Hodgkiss, "The spectral energy distribution of daylight," Br. J. Appl. Phys. **14,** 125–131 (1963).
9. V. D. P. Sastri and S. B. Manamohanan, "Spectral distribution and colour of north sky at Bombay," J. Phys. D **4,** 381–386 (1971).
10. Y. Nayatani, M. Hitani, and H. Minato, "Chromaticity and spectral energy distribution of daylight from north sky at Amagasaki, Japan," Bull. Electrotech. Lab. **31,** 1127–1135 (1967).
11. *Colorimetry*, 2nd ed., CIE Publication No. 15.2 (Central Bureau of the CIE, Vienna, 1986), pp. 70–72.
12. I. Nimeroff and J. A. Yurow, "Degree of metamerism," J. Opt. Soc. Am. **55,** 185–190 (1965).
13. J. L. Simonds, "Application of characteristic vector analysis to photographic and optical response data," J. Opt. Soc. Am. **53,** 968–974 (1963).
14. P. Moon, "Proposed standard solar-radiation curves for engineering use," J. Franklin Inst. **230,** 583–617 (1940).
15. International Standard ISO/CIE 10526, CIE standard colorimetric illuminants (International Organization for Standardization/CIE, Geneva, 1991).
16. Licor Incorporated, 4421 Superior St., P.O. Box 4425, Lincoln, Neb.
17. J. P. S. Parkkinen, J. Hallikainen, and T. Jaaskelainen, "Characteristic spectra of Munsell colors," J. Opt. Soc. Am. A **6,** 318–322 (1989).
18. J. Romero, A. García-Beltrán, and J. Hernández-Andrés, "Linear bases for representation of natural and artificial illuminants," J. Opt. Soc. Am. A **14,** 1007–1014 (1997).